Luminescent Graphene Oxide with a Peptide-Quencher Complex for Optical Detection of Cell-Secreted Proteases by a Turn-On Response

Seon-Yeong Kwak, Jin-Kyoung Yang, Su-Ji Jeon, Hye-In Kim, Joonhyuk Yim, Homan Kang, San Kyeong, Yoon-Sik Lee, and Jong-Ho Kim**

Graphene oxide (GO) is an emerging luminescent nanomaterial with photostable and unique photoluminescence (PL) in the visible and near-infrared region. Herein, a GO PL-based optical biosensor consisting of a luminescent GO donor covalently linked with a peptide-quencher complex is reported for the simple, rapid, and sensitive detection of proteases. To this end, the quenching efficiency of various candidate quenchers of GO fluorescence, such as metalloprotoporphyrins and QXL_{570}, are examined and their quenching mechanisms investigated. A fluorescence resonance energy transfer-based quencher, QXL_{570}, is found to be much more effective for quenching the intrinsic fluorescence of GO than other charge transfer-based quenchers. The designed GO–peptide–QXL system is then able to sensitively detect specific proteases—chymotrypsin and matrix metalloproteinase-2—via a "turn-on" response of quenched GO fluorescence after proteolytic cleavage of the quencher. Finally, the GO–peptide–QXL hybrid successfully detects MMP-2 secreted from living cells—human hepatocytes HepG2—with high sensitivity.

1. Introduction

Proteases are hydrolytic enzymes that break up specific amide bonds in peptides and proteins. At least 500–600 proteases, which are approximately 2% of the human genome, have been identified using bioinformatics.[1,2] Proteases are implicated in multiple normal biological processes and also noticeable in a variety of pathological conditions[3] including cancer,[4] arthritis,[5] and neurodegenerative diseases.[6] For example, matrix metalloproteinases (MMPs) are overexpressed in disease conditions, often in tumor sites,[7] which is a good candidate for a therapeutic target. Therefore, the sensitive, reliable, and convenient detection of proteolytic activity is one of the important issues for early diagnosis and the development of drug-screening systems.[8] Over the past decades, several kinds of methods have been developed for protease detection, based on fluorescence resonance energy transfer (FRET),[9,10] enzyme-linked immunosorbent assay,[11] chemoluminescence,[12] and activity-based labeling.[13] In particular, FRET-based optical sensors, which have a fluorescent donor and an acceptor in close proximity, have received much attention due to their simple fabrication and detection strategy, and high sensitivity. In the standard configuration of FRET sensors, organic fluorophores have generally been used as donors as well as acceptors. However, they suffer from drawbacks such as photo-/chemical degradation, pH susceptibility, and narrow absorption overlapped with broad emission windows.[14] Therefore, there is a crucial need to develop an alternative to conventional organic fluorophores in FRET-based bioassays, which can not only address some of their deficiencies but also improve assay sensitivity and reduce the need for complicated instrumentation.

Graphene oxide (GO), which is a single-layer sheet of carbon material exfoliated by the oxidation of graphite,[15] is a new type of fluorophore that emits strong photoluminescence (PL) in the visible and near-infrared (NIR) regions of the electromagnetic spectrum.[16–20] The wavelength of GO PL, which originates from the recombination of electron–hole pairs in the disrupted π network at oxidation sites, is controllable by varying the density of oxidation in its basal plane.[18] In particular, GO PL shows good stability against photo-/chemical degradation compared to conventional organic fluorophores,[21] which is beneficial for the real-time and quantitative detection of target biomolecules. In addition to its remarkable optical properties, GO has a number of beneficial characteristics such as biocompatibility, large surface area, ease of preparation and chemical modification, and good

Dr. S.-Y. Kwak, S.-J. Jeon, H.-I. Kim, Prof. J.-H. Kim
Department of Chemical Engineering
Hanyang University
Ansan 426–791, Republic of Korea
E-mail: kjh75@hanyang.ac.kr
J.-K. Yang, J. Yim, S. Kyeong, Prof. Y.-S. Lee
School of Chemical and Biological Engineering
Seoul National University
Seoul 141–742, Republic of Korea
E-mail: yslee@snu.ac.kr
H. Kang, Prof. Y.-S. Lee
Interdisciplinary Program in Nano-Science and Technology
Seoul National University
Seoul 151–742, Republic of Korea
DOI: 10.1002/adfm.201400001

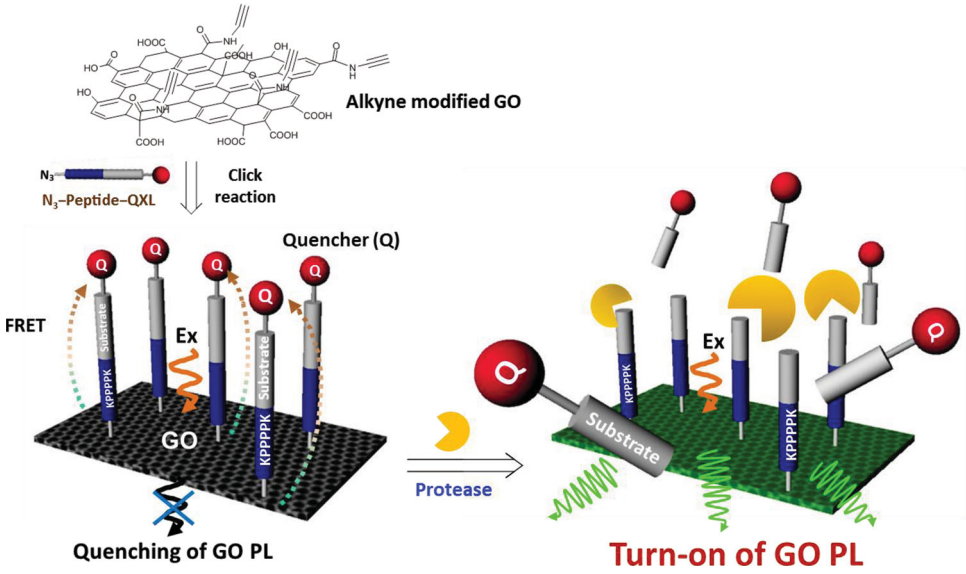

Scheme 1. Schematic illustration for GO-based optical sensor consisting of a luminescent GO donor and a peptide-quencher complex, and the optical detection of protease by the turn-on response of GO fluorescence.

stability as applied in the field of biotechnology and nanomedicine.[22–25] Hence, very recently, GO has been utilized as a fluorescent label for imaging and sensing of biomolecules.[26–28] To date, however, GO has been extensively used as a universal quencher for organic fluorescent dyes rather than as a fluorophore in the current prevailing bioassay systems.[29–36] GO has hardly been explored as an emitting fluorophore (donor) for signal transduction in FRET-based bioassay systems, although it exhibits outstanding fluorescence properties. Therefore, it is of great interest to develop the pair of a GO fluorescent donor and its quencher as a FRET-based bioassay platform for the detection of various biological molecules, since the use of GO PL with unique photophysical properties will be helpful to address some of the deficiencies that conventional organic fluorophores have shown in bioassays. In order to exploit GO as an emitting donor in FRET-based bioassays, the screening of effective quenchers for GO PL is required, and the quenching mechanism should be understood to design an efficient biosensor for the detection of desired targets.

Herein, we demonstrate a novel GO-based sensing platform, which consists of a luminescent GO donor and a peptide-quencher complex, for the simple and selective detection of proteases through the turn-on response of inherent GO PL (**Scheme 1**) upon proteolytic cleavage of the quencher. To design the most effective pair as a GO-based FRET system, various quencher candidates for GO PL such as metalloprotoporphyrin derivatives (MePPs) and QXL_{570} were screened to evaluate their quenching efficiency, and the quenching mechanism was investigated. The designed GO-peptide–quencher hybrids were able to selectively and specifically detect chymotrypsin and matrix metalloproteinase-2 (MMP-2) by the recovery of quenched GO PL arising from the cleavage of the substrate peptide–quencher complex. Finally, we successfully applied the GO-peptide–quencher hybrid to detect MMP-2 secreted from living cells, human hepatocytes HepG2.

2. Results and Discussion

2.1. Study of Quenching of GO PL

As-prepared GO showed unique optical properties (see Figure S1 of the Supporting Information). In UV absorption spectra, GO had two characteristic peaks at 230 and 300 nm originating from the π–π^* transition of the C=C bond and the n–π^* transition of the C=O bond.[27] Also, an intense fluorescence emission peak at 543 nm was observed under 400 nm excitation, which results from the recombination of electron–hole pairs localized within a diminutive sp^2 domain embedded in an sp^3 matrix.[37] This emission property allows the use of GO as a fluorescent donor in the FRET-based detection of proteases.

To find an effective quencher for GO fluorescence, we selected several metalloprotoporphyrin derivatives (MePPs) and QXL_{570} in terms of two possible quenching mechanisms: charge transfer and FRET from GO to a quencher, respectively. Initially, we assumed that several MePPs such as zinc (Zn^{2+}) protoporphyrin (ZnPP), iron (Fe^{2+}) protoporphyrin (FePP), copper (Cu^{2+}) protoporphyrin (CuPP), and cobalt (Co^{3+}) protoporphyrin chlorides (CoPP) could quench GO fluorescence via charge transfer from GO to the metal ions, in which the protoporphyrin structure could enhance their quenching efficiency by putting them in a close proximity to the GO surface through π–π interactions. Moreover, we expected that QXL_{570} could play a role as a dark quencher since its absorption largely overlapped with the maximum position of GO fluorescence (543 nm at 400 nm excitation).

As shown in **Figure 1**a, the addition of MePPs and QXL_{570} to the GO solution induced an instantaneous decrease in GO fluorescence at 400 nm excitation. GO fluorescence gradually decreased with increasing the concentration of the quenchers from 10 to 50 μM (Figure S2). Their quenching efficiency ($\Delta I_{543\ nm}$) increased linearly at this range of quencher concentrations, which is perfectly consistent with the Stern–Volmer equation (Figure 1b)

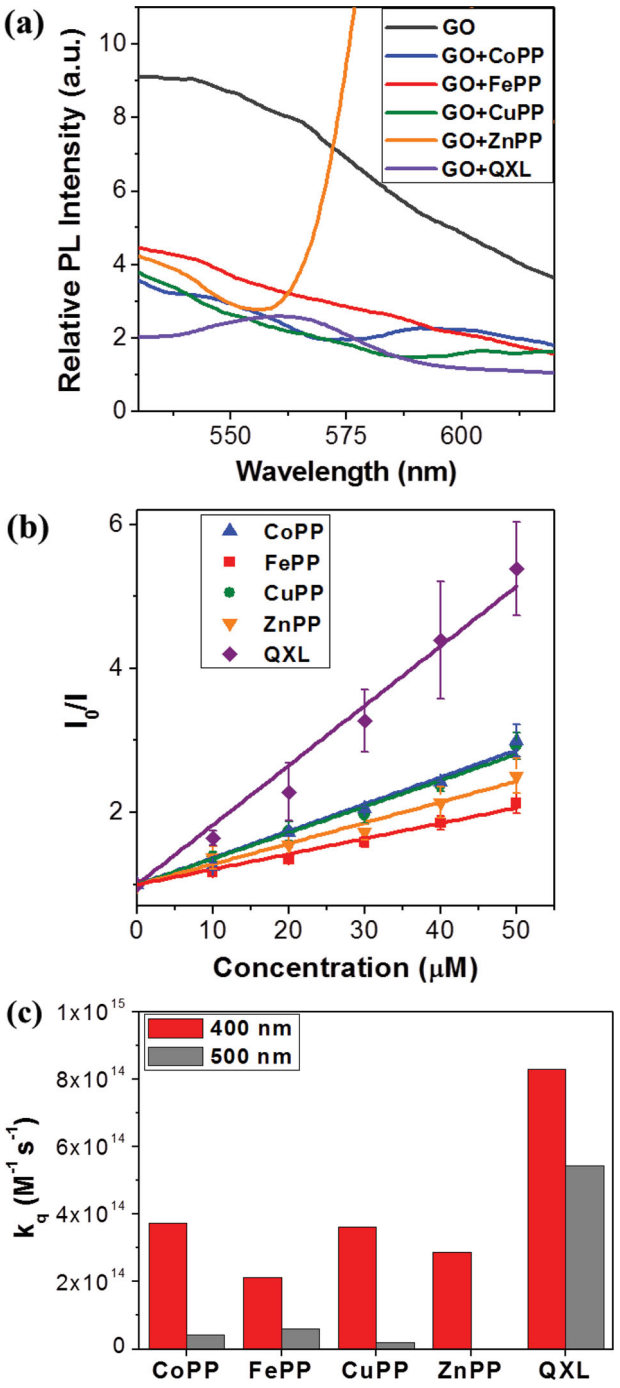

Figure 1. Screening of effective quencher for GO PL. (a) Fluorescence spectra of a GO solution (0.1 mg/mL) in the presence of MePPs and QXL_{570} (50 μM) under excitation at 400 nm. (b) Stern–Volmer plot for GO fluorescence quenching by MePPs and QXL_{570} measured under excitation at 400 nm, showing linear fit to the Stern–Volmer equation. (c) Quenching rate constants of MePPs and QXL_{570} for GO fluorescence measured under excitation at 400 and 500 nm. All error bars represent standard deviation from the mean.

$$I_0 / I = K_{sv}[Q] + 1 = k_q \tau_0 [Q] + 1$$

where I_0 is the intensity of GO fluorescence in the absence of a quencher, I is the intensity of GO fluorescence in the presence of a quencher, [Q] is the quencher concentration, K_{sv} is the Stern–Volmer quenching constant, k_q is the quenching rate constant, and τ_0 is the lifetime of GO fluorescence.

Moreover, we calculated the quenching rate constants for the quenchers as shown in Figure 1c. QXL_{570} showed the highest quenching constant, twice higher than other MePP quenchers, at 400 nm excitation (red bars). This effective quenching by QXL_{570} is clearly ascribed to FRET from the GO fluorescent donor to the QXL acceptor. As shown in Figure S3, the absorption spectrum of QXL_{570} largely overlapped with the emission fluorescence of GO. MePP derivatives also showed good quenching efficiency. The quenching of GO PL by MePPs mainly arose from their absorption of incident photons, not from charge transfer, since their absorption wavelength exactly matches with an excitation wavelength of 400 nm (Figure S3), which results in a significant decrease in the number of photons coming to GO. Therefore, we varied the excitation wavelength from 400 nm to 500 nm and calculated the quenching rate constant for all quenchers. As shown in Figure 1c (grey bars), the quenching efficiency of MePP derivatives significantly decreased, but still showed a moderate quenching effect through charge transfer from GO to the metal ions.[38,39] In contrast, QXL_{570} maintained great quenching efficiency of the GO fluorescence even at 500 nm excitation. The small decrease in its quenching constant is attributed to the higher extinction coefficient of QXL_{570} at 500 nm. This result indicates that the quenching of GO fluorescence by FRET is much more effective than by charge transfer. From this quenching study, we concluded that QXL_{570} was the most efficient quencher for GO fluorescence, with the highest quenching constants regardless of excitation wavelength. Therefore, we chose QXL_{570} as a quencher for further studies on a GO-based optical sensor for protease detection.

2.2. Peptide Design for Chymotrypsin and MMP-2

The peptide substrates for chymotrypsin and MMP-2 were rationally designed to impart several functions. The tetra-proline (PPPP) sequence was included as a stretchable rigid spacer for the peptide substrates to provide clear exposure of a protease cleavage site. In addition, two lysines (K, K) were introduced to make GO–peptide–QXL hybrids more hydrophilic and well-dispersible in aqueous solutions to avoid aggregation. Cysteine was also included at the *C*-terminal of peptides to attach QXL_{570} through the reaction of thiol with maleimide. Then, an azide group was coupled to the *N*-terminal of the peptides to functionalize the GO bearing an alkyne group through Click chemistry, which gives rise to the formation of GO–peptide–QXL hybrids. Finally, the active amino acid residues for specific protease recognition such as chymotrypsin and MMP-2 were introduced to the middle of the peptides.

We chose chymotrypsin and MMP-2 as model enzymes since chymostrypsin is a well-characterized protease and MMP-2 is one of the most important pharmaceutical target enzymes. Chymotrypsin is a serine protease that hydrolyzes peptide bonds at the *C*-terminal, containing hydrophobic or aromatic side chains such as phenylalanine. We designed two different peptides: one is Ala-Ala-Pro-Phe (AAPF), which has a chymotrypsin cleavage

site, and the other is a control sequence, tetraglycine (GGGG), which cannot be cleaved by chymotrypsin, to prove the specificity of our optical sensor. MMP-2 is often overexpressed in tumors and is deeply involved in cancer metastasis by allowing extravasation and invading tumor cells to normal tissues.[4,40,41] MMP-2 specifically cleaves the *N*-terminal to Gly in Gly-Pro-Leu-Gly-Val-Arg-Gly[42] (GPLGVRG). Therefore, we introduced these peptide sequences to the peptide–QXL complex.

2.3. GO–Peptide–QXL Hybrids for Optical Detection of Proteases

To synthesize GO–peptide–QXL biosensors for the detection of chymotrypsin and MMP-2, GO was first functionalized with chloroacetic acid to increase the number of carboxylic acid groups on its surface (CMGO).[27,43] Then, propagylamine was coupled to the carboxylic acid groups of CMGO to introduce alkyne groups on its surface (alkyne GO). Thus, N_3-peptide was conjugated to the alkyne groups on alkyne GO through Click chemistry to obtain the GO–peptide conjugates (GO–peptide). QXL_{570}-maleimide was then simply reacted with the thiol group of cysteine on the GO–peptide conjugates (GO–peptide–QXL). The obtained GO–peptide–QXL hybrids were characterized by atomic force microscopy (AFM), Fourier transform infrared (FT-IR) spectroscopy, and elemental analysis. The AFM images and the height profiles revealed that GO had a height of ~2 nm (**Figure 2**a), whereas GO–peptide–QXL had a height of around 15 nm (Figure 2b), which indicates that the peptide–QXL complexes were successfully coupled to GO. We also analyzed the structure of GO–peptide–QXL hybrids using FT-IR spectroscopy. As shown in Figure 2d, the vibrational modes for an amide carbonyl group (C=O 1635 cm^{-1}) and a triazole group (C=N 1529 cm^{-1}, C–N 1323 cm^{-1}) in GO–peptide–QXL were distinctly observed, as compared with GO (Figure 2c) and CMGO (Figure S4a). In addition, the elemental analysis of GO–peptide–QXL hybrids showed an increase in the nitrogen content (11.5 wt%) compared to GO, CMGO, and alkyne-GO, as shown in Figure S4b. Lastly, we measured the fluorescence of GO–peptide–QXL. The fluorescence of GO decreased after coupling QXL_{570} to the peptides on GO (Figure S4c). These analytical results clearly demonstrate the successful formation of GO–peptide–QXL hybrid sensors.

We then investigated the performance of GO–peptide–QXL hybrids for the detection of chymotrypsin and MMP-2. First, the activities of GO–peptide–QXL hybrid sensors were evaluated for chymotrypsin. **Figure 3**a shows the structures of two sensors: GO–peptide 1–QXL, bearing a specific peptide sequence (AAPF), and GO–peptide 2–QXL bearing a control peptide sequence (GGGG). As shown in Figure 3b, the original fluorescence intensity of GO–peptide 1–QXL was very low due to the quenching by QXL_{570} via FRET. Quenched fluorescence of GO–peptide 1–QXL was restored only when chymotrypsin was added. The fluorescence intensity gradually increased with increasing the concentration of the protease from 5 to 500 mU mL^{-1}. However, GO–peptide 2–QXL, which contains no specific peptide sequence of chymotrypsin, did not restore its quenched fluorescence even after chymotrypsin was added (Figure 3c). These results clearly suggest that the designed GO–peptide 1–QXL was able to selectively recognize the presence of chymotrypsin. In addition, its response kinetics was so fast that the sensor recognized the target within 10 min (Figure 3d). For more rigorous study on the kinetics of the analytical performance, we measured the rates for the fluorescence response of the GO–peptide 1–QXL to chymotrypsin to obtain a Michaelis constant (K_m) and a maximum rate (V_{max}). The Lineweaver–Burk plot showed (Figure S5) that K_m and V_{max} appeared to be 0.16 μM and 0.15 min^{-1}, respectively, which suggest that the detection kinetics of the GO–peptide 1–QXL sensor was very fast.

We further confirmed whether or not the restoration of the quenched fluorescence in GO–peptide 1–QXL was due to the cleavage of the peptide-QXL through mass spectrometry (MS) analysis. As shown in Figure S6a, after the addition of chymotrypsin to GO–peptide 1–QXL, the hydrolyzed peptide-QXL fragment (C(QXL)-NH_2) with consistent mass (996.3) was detected in the mass spectra, while no other fragments were detected from GO–peptide 2–QXL (negative control) after chymotrypsin treatment (Figure S6b). In other cases such as GO–peptide 1–QXL or GO–peptide 2–QXL without adding chymotrypsin, no extra mass fragment was observed (Figure S6c and S6d) as expected. These MS analysis results exhibit that the fluorescence turn-on in the GO–peptide 1–QXL sensor was caused by the cleavage of the peptide–QXL by chymotrypsin. Next, we investigated the effect of a chymotrypsin inhibitor on the fluorescence restoration of the sensor. As the chymotrypsin inhibitor, phenylmethanesulfonyl fluoride, was added with the enzyme to the solution of GO–peptide 1–QXL, the degree of fluorescence restoration substantially decreased depending on the concentration of the inhibitor from 10 to 125 μM (Figure 3e). This result supports that the sensor could be used for the screening of inhibitors to other proteolytic enzymes.

Then, we evaluated the performance of GO–peptide 3–QXL designed for sensing MMP-2. **Figure 4**a shows the structure of the sensor platform. The quenched fluorescence of the GO–peptide 3–QXL sensor was restored after the addition of MMP-2 and the fluorescence recovery increased with increasing the concentration of the protease (Figure 4b). However, no fluorescence recovery was observed in the control experiment where GO–peptide 3–QXL was treated with chymotrypsin (Figure 4c). These results obviously suggest that the GO–peptide 3–QXL sensor was able to detect the specific protease MMP-2 through the turn-on response of the quenched fluorescence. We then measured the rates for the fluorescence response of the GO–peptide 3–QXL sensor to MMP-2 to obtain the values of K_m and V_{max}. After the linear regression of the Lineweaver–Burk plot (Figure S7), 0.76 μM for K_m and 0.49 min^{-1} for V_{max} were obtained, which suggest that the sensing kinetics of the GO–peptide 3–QXL sensor for MMP-2 was very fast as well. In addition, MS analysis confirmed that the restoration of the quenched fluorescence in GO–peptide 3–QXL was caused by the proteolytic cleavage of the peptide–QXL by MMP-2. The hydrolyzed peptide sequence, H–VRGC(QXL)–NH_2, was detected in the MS data (Figure S8). Next, we investigated the effect of the MMP-2 inhibitor, prinomastat hydrochloride, on the fluorescence response of the sensor. When the MMP-2 inhibitor was added together with the protease into the solution of GO–peptide

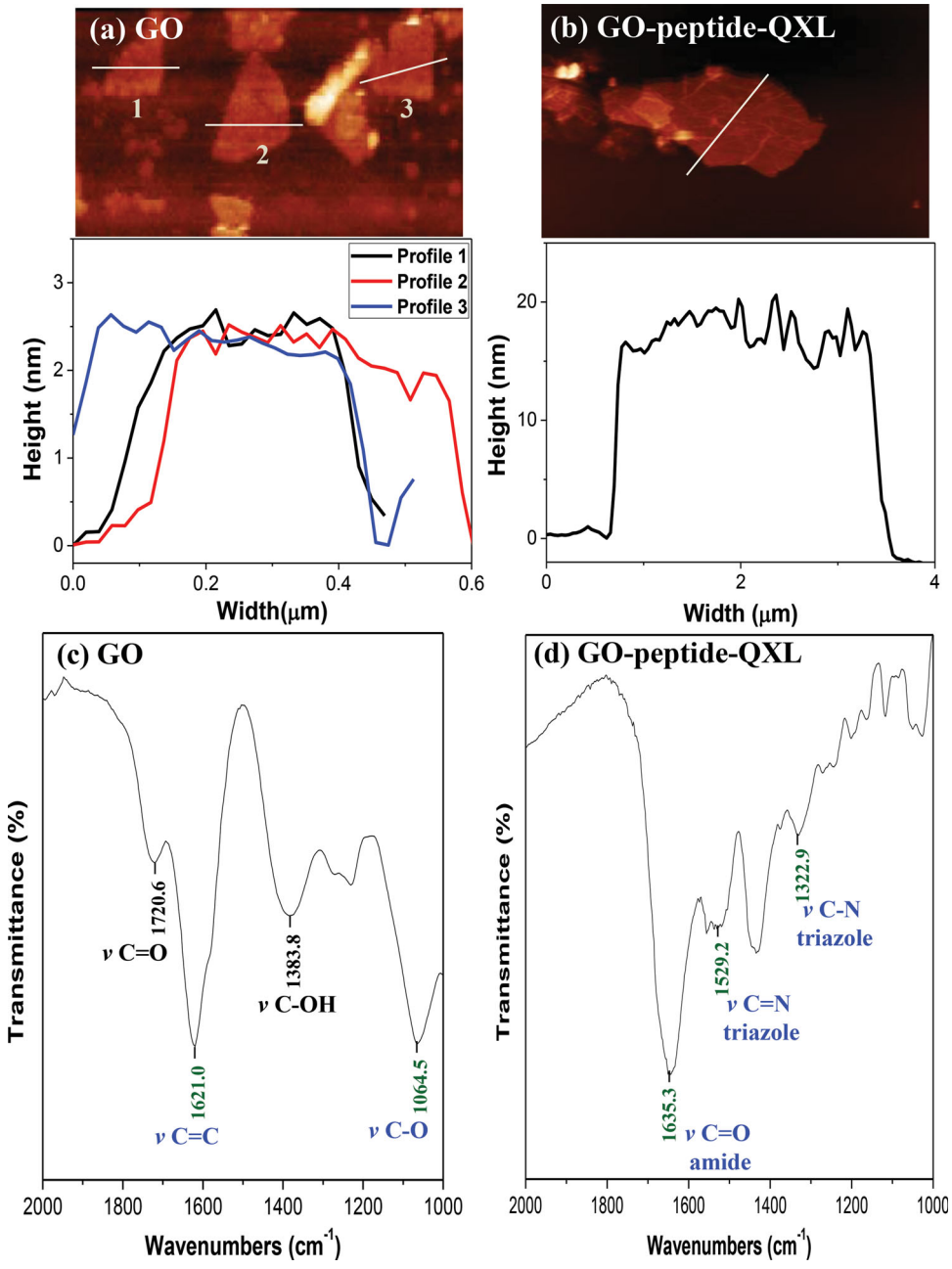

Figure 2. Characterization of GO–peptide–QXL hybrid. (a) AFM image and height profiles of GO and (b) GO–peptide 1–QXL. (c) FT-IR spectra of GO and (d) GO–peptide 1–QXL.

3–QXL, the restoration rate of the quenched fluorescence significantly decreased depending on the inhibitor concentration from 10 to 100 μM (Figure 4d).

GO–peptide–QXL hybrids for the detection of the proteases exhibited superior stability for long-term storage. We found that GO–peptide–QXL hybrids could perfectly maintain the quenching activity of fluorescence for 30 days at 25 °C in water, and GO fluorescence was successfully recovered by the proteolytic cleavage of the quencher even after 30 days (Figure S9). We speculate that this stability may arise from covalent bonding between GO and QXL which prevents the peptide probes from being released from the GO surface during storage. Thus, the GO–peptide–QXL hybrid proved to be a more suitable biosensor for various biomedical applications, compared to other biosensors based on the physical adsorption of probe ligands and organic fluorescent dyes.

2.4. Detection of MMP-2 Secreted from Living Cells

Finally, we applied the GO–peptide 3–QXL sensor for the detection of MMP-2 secreted from living cells. MMP-2

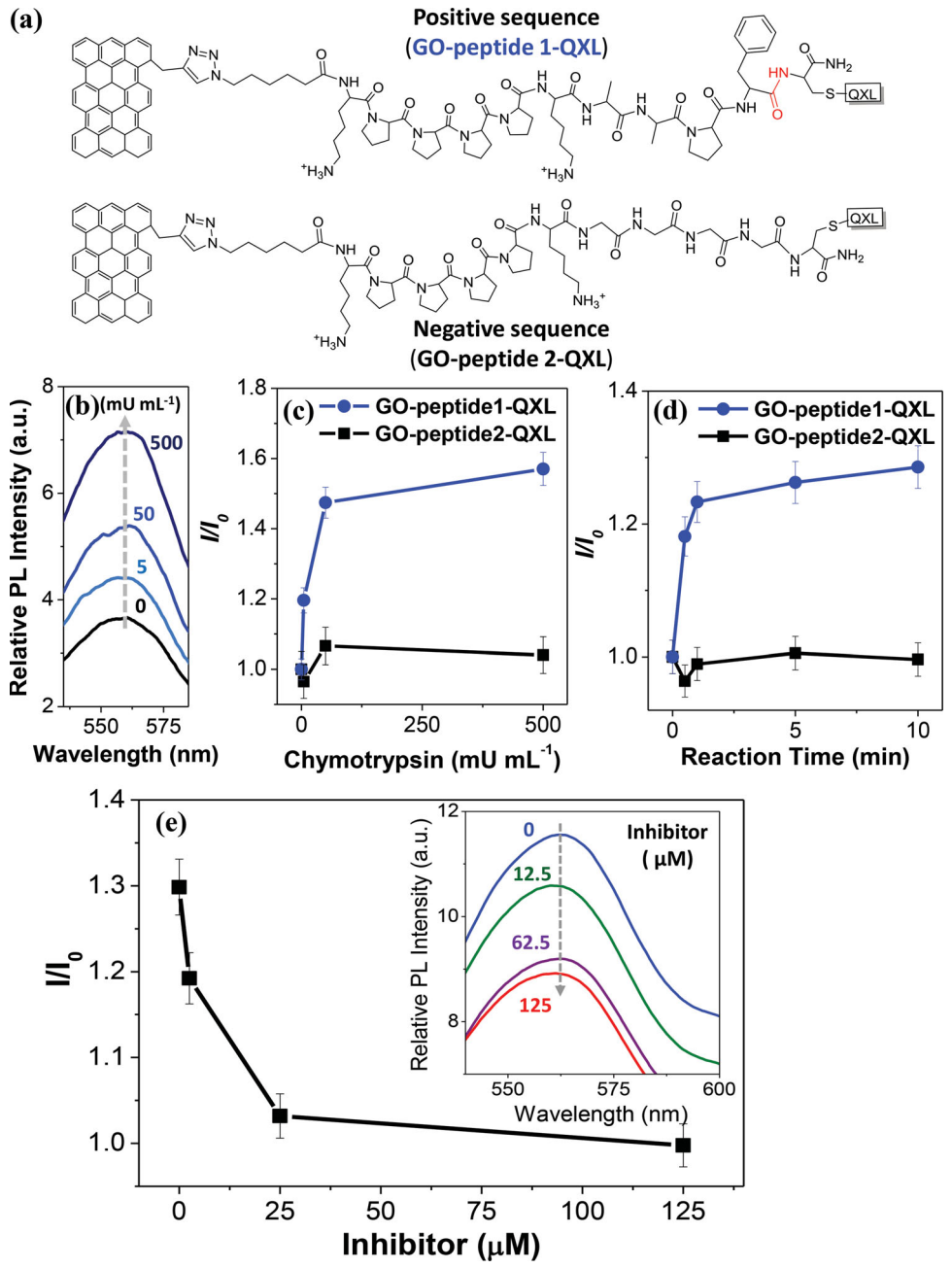

Figure 3. Optical detection of chymotrypsin with GO–peptide–QXL hybrid. (a) Chemical structure of GO–peptide 1–QXL for chymotrypsin detection and the negative control sensor (GO–peptide 2–QXL). The red color indicates the cleavage site by chymotrypsin. (b) Fluorescence response of GO–peptide 1–QXL to chymotrypsin at various concentrations (0, 5, 50, and 500 mU mL^{-1}). (c) Quantitative analysis of fluorescence recovery (at 560 nm) in GO–peptide 1–QXL and GO–peptide 2–QXL as a function of chymotrypsin concentrations. (d) Quantitative analysis of fluorescence recovery (at 560 nm) in GO–peptide 1–QXL and GO–peptide 2–QXL as a function of reaction time in the presence of chymotrypsin (50 mU mL^{-1}). (e) Effect of a chymotrypsin inhibitor on the fluorescence recovery of GO–peptide 1–QXL at 560 nm in the presence of chymotrypsin (50 mU mL^{-1}): the concentration of a chymotrypsin inhibitor (phenylmethanesulfonyl fluoride) was varied from 0, 12.5, and 62.5 to 125 μM, and the inset presents the fluorescence spectra of GO–peptide 1–QXL at each inhibitor concentration. I_0 and I are the fluorescence intensity without and with chymotrypsin. All error bars represent standard deviation from the mean.

detection in a biological environment is important for the diagnosis and therapy of cancers at an early stage. We could detect MMP-2 secreted from human liver hepatocellular carcinoma cells, HepG2 (**Figure 5**a), using GO–peptide 3–QXL. The recovery of fluorescence intensity was calculated by the following equation:

$$\text{Recovery of PL} = \frac{I}{I_0} - 1$$

where I is the fluorescence intensity after the incubation of GO–peptide 3–QXL in the HepG2 cell-cultured media for 30 min, and I_0 is the fluorescence intensity after the incubation

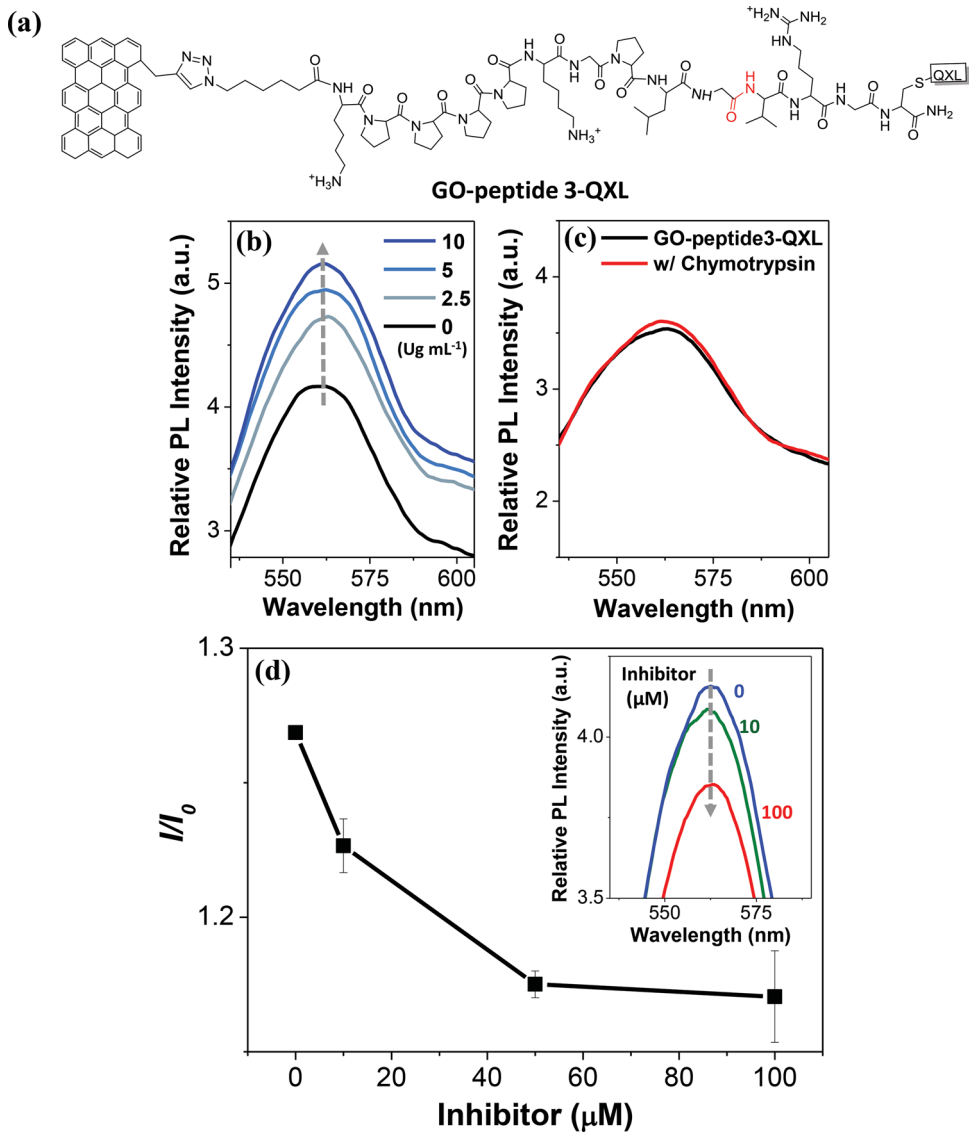

Figure 4. Optical detection of MMP-2 with GO–peptide 3–QXL hybrid. (a) Chemical structure of GO–peptide 3–QXL hybrid for detection of MMP-2. The red color indicates the cleavage site by MMP-2. (b) Fluorescence response of GO–peptide 3–QXL to MMP-2 at various concentrations (0, 2.5, 5, and 10 Ug mL^{-1}). (c) Fluorescence response of GO–peptide 3–QXL to chymotrypsin (50 mU mL^{-1}). (d) Effect of a MMP-2 inhibitor on the fluorescence recovery of GO–peptide 3–QXL at 560 nm in the presence of MMP-2 (5 Ug mL^{-1}): the concentration of a MMP-2 inhibitor (Prinomastat hydrochloride) was varied from 0, 10, to 100 μM, and the inset presents the fluorescence spectra of GO–peptide 3–QXL at each inhibitor concentration. I_0 and I are the fluorescence intensity without and with MMP-2. All error bars represent standard deviation from the mean.

of GO–peptide 3–QXL in the cell-free media for 30 min. As expected, MMP-2 would be secreted in the HepG2 cell-cultured media, while there would be no MMP-2 in the cell-free media. First, we quantified the amount of MMP-2 secreted from the cells using a gold standard enzyme-linked immunosorbent assay (ELISA) method. The amount of human MMP-2 secreted from HepG2 cells increased as a function of cell culture time (green line in Figure 5b). After cell incubation for 48 h, 3.7 ng mL^{-1} of MMP-2 was secreted from the cells. At the same time intervals with an ELISA test, the fluorescence response of GO–peptide 3–QXL was measured. The quenched fluorescence of the sensors was gradually restored with increasing the cell incubation time (blue line in Figure 5b), indicating that the amount of secreted MMP-2 increased. This turn-on response of GO fluorescence correlated well with the concentration of MMP-2 measured by ELISA, and the detection limit of the GO–peptide 3–QXL sensor was 2.0 ng mL^{-1}, which is lower than the previously reported one with MMP-2 FRET sensors.[44–46] To confirm that this turn-on response was caused by MMP-2 secreted from the cells, the cell-cultured media was pre-incubated with 50 μM of MMP-2 inhibitor, followed by addition of the GO–peptide 3–QXL sensor. As shown in Figure 5c (orange bar), a substantially decreased response was observed, which verifies that the turn-on response was caused by MMP-2 secreted from HepG2 cells. Finally, we conducted one more control experiment to demonstrate the

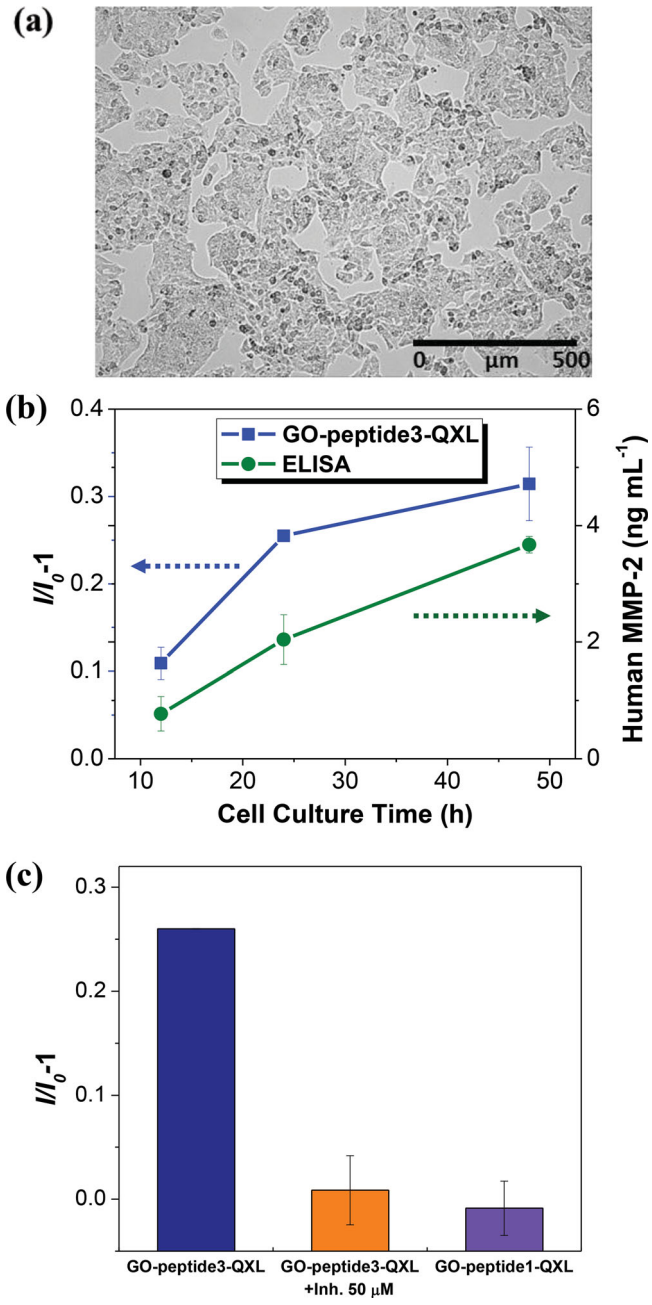

Figure 5. In-vitro detection of MMP-2 secreted from living cells with GO–peptide 3–QXL. (a) Optical image of HepG2 cells. (b) Fluorescence response (blue line) of GO–peptide 3–QXL to MMP-2 secreted from HepG2 as a function of cell culture time (12, 24, and 48 h): the concentration of MMP-2 secreted from HepG2 was measured by ELISA (green line). (c) Effect of a MMP-2 inhibitor (50 μM) on the fluorescence response of GO–peptide 3–QXL to secreted MMP-2 (orange bar), and the fluorescence response of GO–peptide 1–QXL (0.1 mg mL^{-1}) to secreted MMP-2 (purple bar). I_0 and I indicate the fluorescence intensity after incubation of cell-free media and HepG2 cell-cultured media, respectively. All error bars represent standard deviation from the mean.

specificity of the GO–peptide 3–QXL sensor for MMP-2. GO–peptide 1–QXL (0.1 mg mL^{-1}) bearing a peptide sequence, which is not cleaved by MMP-2, was treated with HepG2 cell culture media under the same conditions. As shown in Figure 5c, no valid fluorescence turn-on response was observed (purple bar), verifying that the GO–peptide 3–QXL specifically responded to MMP-2. These results clearly confirmed that the cell-secreted MMP-2 was successfully detected by the turn-on response of our GO–peptide–QXL system.

3. Conclusion

We have constructed a new GO-based optical biosensor consisting of luminescent GO and covalently linked peptide-quencher complexes, which can detect protease activity specifically with high sensitivity. In this FRET-based sensing system, GO was used as both an emitting fluorophore and a scaffold for attaching peptide-quencher complexes. We designed GO-peptide-quencher hybrids while considering the quenching efficiency of MePPs and QXL_{570} on GO PL, and investigated their quenching mechanism based on charge or energy transfer. The designed GO–peptide–QXL hybrids revealed their selectivity for the detection of chymotrypsin and MMP-2 in vitro assay by the "turn-on" response of inherent GO fluorescence. Eventually, the GO–peptide–QXL sensor was applied to a real biosystem as a "turn-on" sensor for the detection of MMP-2 secreted from HepG2 cells with high sensitivity. This GO-based FRET sensing platform has a great potential for the detection of various biological molecules in extensive fields including clinical diagnostics, pharmaceutical screening, and medical research.

4. Experimental Section

Screening of Effective Quencher for GO: GO was synthesized from graphite flakes using a modified Hummers method.[15] Graphite was oxidized in H_2SO_4 and $KMnO_4$, and subsequently sonicated for 1.5 h at 12 W in an ice-bath. After centrifugation, GO was intensively washed with H_2O. As-synthesized GO aqueous solution (2.3 mg mL^{-1}) was diluted with phosphate buffer (0.1 M, pH 7.0) to 0.1 mg mL^{-1}. MePPs and QXL_{570} were dissolved in DMSO and added to the GO solution. The final concentration of the quencher molecules was varied from 10 to 50 μM. After gentle mixing, the fluorescence of GO was measured by a fluorescence spectrometer (LS-55, PerkinElmer, MA, USA) using 400 nm-excitation and 1.0 s integration time.

Preparation of GO–Peptide–QXL Hybrids: Peptides were synthesized by conventional solid-phase synthesis method using an Fmoc/tBu strategy on Rink amide MBHA resin (0.40 mmol g^{-1}). After the protease substrate peptides with proline linker were completely synthesized, azidohexanoic acid (2 equiv.), BOP (2 equiv.), HOBt (2 equiv.), and DIPEA (4 equiv.) were added to the peptide-anchored resin in NMP, and the coupling reaction proceeded for 2 h at room temperature. The resulting N_3-peptides were cleaved from the resin support by treating with a cleavage cocktail containing TFA/anisole/DODT/TIPS (95.5/2/1.5/1%) for 2 h. The resin was filtered, and then washed with TFA, DCM and methanol. The filtrate and washings were combined, concentrated under high vacuum, and then precipitated with cold diethyl ether to obtain the N_3-peptides as a white powder. The precipitates were then centrifuged at 7000 rpm for 3 min and washed with diethyl ether five times. The crude N_3-peptides were further purified using semi-preparative RP-HPLC (Thermo Scientific Spectra System AS3000; Thermo-Fisher, Waltham, MA) with an A to B gradient (A: 0.1% TFA in water, B: 0.1% TFA in acetonitrile; from 10% to 90% B over 30 min, at a flow rate of 4.0 mL min^{-1}) and freeze-dried. The resulting N_3-peptides were identified by a QUATTRO triple quadrupole tandem mass spectrometer (Waters Micromass, MA, USA).

Chloroacetic acid was reacted with GO to introduce more carboxylic groups on the GO surface. Five milliliters of GO solution (2.3 mg mL^{-1}) was dispersed in 5 mL of 6 M NaOH solution. A 1.46 g portion of chloroacetic acid was added to the GO solution in an ice bath. The temperature was raised up to 60 °C, and then the reaction mixture was magnetically stirred for 1.5 h. After cooling down, carboxymethylated GO (CMGO) was centrifuged at 15 000 rpm for 40 min, and washed with water several times until the pH of the CMGO solution became pH 5.4. Then, propagyl amine (10 equiv.) was coupled to the carboxylic group of CMGO using EDC/NHS (10 equiv.) in phosphate buffer (0.1 M, pH 6.0) for 3 h at room temperature to introduce an alkyne group.

For the preparation of GO–peptide–QXL hybrids as a chymotrypsin sensor, 'N_3-peptide 1' (1 equiv.), and 'N_3-peptide 2' (1 equiv.) were conjugated to alkyne-modified GO through triazole linkage by Click chemistry with $CuSO_4$_$5H_2O$ (3 equiv.) and sodium ascorbic acid (8.5 equiv.) in phosphate buffer (0.1 M, pH 7.0) for 18 h at 25 °C. Then, the resulting GO–peptide–QXL hybrids were washed with water several times to remove the unreacted peptides. Next, QXL_{570} C2 maleimide (1 equiv.) was coupled to the thiol group at the *C*-terminal of GO-peptide conjugates in DMSO for 2 h. GO–peptide–QXL hybrids were washed with DMSO and water several times. For the preparation of the GO–peptide 3–QXL hybrid for MMP-2, the MMP-2 substrate peptide (N_3-peptide 3, 1 equiv.) was first reacted with QXL_{570} C2 maleimide (1 equiv.) in a mixture of phosphate buffer (0.1 M, pH 7.0) and DMSO for 2 h. N_3-peptide 3-QXL (1 equiv.) was then coupled to alkyne-modified GO in the presence of $CuSO_4$_$5H_2O$ (3 equiv.) and sodium ascorbic acid (8.5 equiv.) in phosphate buffer (0.1 M, pH 7.0) for 18 h at 25 °C. GO–peptide 3–QXL hybrid was washed with water several times.

Detection of Chymotrypsin and MMP-2: Chymotrypsin was added to GO–peptide 1–QXL or GO-peptide-2-QXL (0.1 mg mL^{-1}) in Tris-HCl buffer (0.1M, pH 7.8), and the reaction mixture was incubated for 10 min at 25 °C. The final concentration of chymotrypsin was varied from 0 to 500 mU mL^{-1}. Then, the fluorescence response was measured with 400 nm-excitation and 1.0 s integration time. For the effect of an inhibitor, the inhibitor was pre-incubated with chymotrypsin (50 mU mL^{-1}) in Tris-HCl buffer (0.1M, pH 7.8) for 10 min at 25 °C, and then added to the GO–peptide 1–QXL solution (0.1 mg mL^{-1}). For testing with MMP-2, MMP-2 was added to GO–peptide 3–QXL (0.1 mg mL^{-1}) in Tris-HCl buffer (50 mM, pH 7.6), and the reaction mixture was incubated for 30 min at 37 °C. The final concentration of MMP-2 was varied from 0 to 10 Ug mL^{-1}. For the effect of an inhibitor, the inhibitor was pre-incubated with MMP-2 (5 Ug mL^{-1}) for 10 min at 37 °C, and then added to the GO–peptide 3–QXL solution (0.1 mg mL^{-1}). For the specificity test of GO–peptide 3–QXL against MMP-2, a different protease, chymotrypsin (0.05 U mL^{-1}) was added into GO–peptide 3–QXL (0.1 mg mL^{-1}) in Tris-HCl buffer (0.1 M, pH 7.8) for 1 h at 25 °C. The relative PL intensity at 560 nm was obtained with 400 nm excitation and 1.0 s integration time.

Detection of MMP-2 Secreted from Living Cells: HepG2 cells were seeded in 10-cm dishes at a density of 2×10^6 cells per dish and cultured in RPMI 1640 containing 10% FBS and 1% peniciline-streptomycin until the cell confluence reached 60%. After replacing with a fresh medium, the cells were incubated for specific time intervals of 12, 24, and 48 h, and then the cell culture supernatant was taken out at each interval to mix with the GO–peptide 3–QXL sensor (0.1 mg mL^{-1}) for 30 min at 37 °C with gentle shaking (approximately 100 rpm). The fluorescence response of the sensor was measured by a fluorescence spectrometer (NanoLog, HORIBA Co. Ltd., Kyoto, Japan) with 400 nm excitation and 0.01 sec exposure time. In addition, the concentration of MMP-2 secreted from the cells was determined by a MMP-2 Human ELISA kit (Abcam, Cambridge, UK). A 100 µL portion of each standard and sample were added into human MMP-2 specific antibody coated wells. After incubation for 2.5 h at 25 °C with gentle shaking, the solution was completely removed. A 100 µL portion of biotinylated MMP-2 detection antibody was added to each well, and incubated for 1 h at 25 °C with gentle shaking. The solution was discarded, then a 100 µL of HRP-Streptavidin solution was added in each well for 45 min at 25 °C with gentle shaking. The washing step was repeated, and then a 100 µL of TMB one-step substrate reagent was added to each well, and incubated for 30 min at 25 °C in the dark with gentle shaking. Absorbance was measured at 450 nm by a microplate spectrophotometer (MQX200R, BioTek Instruments, Inc., VT, USA) immediately after adding 50 µL of stop solution. A new standard curve was generated for each assay, and each sample was assayed in duplicates. In addition, control experiments were carried out for MMP-2 sensor. MMP-2 inhibitor (50 µM) was added to HepG2 cells culture media, and pre-incubated at 37 °C for 30 min. GO–peptide 3–QXL (0.1 mg mL^{-1}), MMP-2 sensor, was treated and further incubated at 37 °C for 30 min for enzyme reaction. GO–peptide 1–QXL sensor (0.1 mg mL^{-1}) was incubated with the same HepG2 cell culture media for 30 min at 37 °C with gentle shaking. Control experiment was performed in triplicate.

Supporting Information

Supporting Information is available from the Wiley Online Library or from the author.

Acknowledgements

S.-Y. Kwak and J.-K. Yang contributed equally to this work. HepG2 cells were kindly provided by Professor Miran Seo from College of Medicine, Yonsei University. This work was supported by the Pioneer Research Center Program (Grant Number 2012–0000448), the Science Research Program (Grant Number 2008–0061860), and the Basic Science Research Program (Grant Number 2012-R1A1A1012516, and 2008-0061891) through the National Research Foundation of Korea funded by the Ministry of Science, ICT & Future Planning.

Received: January 1, 2014
Revised: April 12, 2014
Published online: June 20, 2014

[1] N. D. Rawlings, D. P. Tolle, A. J. Barrett, *Nucleic Acids Res.* **2004**, *32*, D160–D164.
[2] X. S. Puente, L. M. Sánchez, C. M. Overall, C. López-Otín, *Nat. Rev. Genetics* **2003**, *4*, 544–558.
[3] C. López-Otín, J. S. Bond, *J. Biol. Chem.* **2008**, *283*, 30433–30437.
[4] J. M. Freije, M. Balbín, A. M. Pendas, L. M. Sanchez, X. S. Puente, C. López-Otín, *New Trends in Cancer for the 21st Century*, Springer, Spain **2003**, pp.91–107.
[5] N. N. Nalivaeva, L. R. Fisk, N. D. Belyaev, A. J. Turner, *Curr. Alzheimer Res.* **2008**, *5*, 212–224.
[6] G. Murphy, H. Nagase, *Nat. Clin. Pract. Rheumatol.* **2008**, *4*, 128–135.
[7] Y. Chau, R. F. Padera, N. M. Dang, R. Langer, *Int. J. Cancer* **2006**, *118*, 1519–1526.
[8] B. Turk, *Nat. Rev. Drug Discov.* **2006**, *5*, 785–799.
[9] N. P. Mahajan, D. Corinne Harrison-Shostak, J. Michaux, B. Herman, *Chem. Biol.* **1999**, *6*, 401–409.
[10] S. M. Rodems, B. D. Hamman, C. Lin, J. Zhao, S. Shah, D. Heidary, L. Makings, J. H. Stack, B. A. Pollok, *Assay Drug Dev. Technol.* **2002**, *1*, 9–19.
[11] L. Kjeldsen, O. W. Bjerrum, D. Hovgaard, A. H. Johnsen, M. Sehested, N. Borregaard, *Eur. J. Haematol.* **1992**, *49*, 180–191.
[12] J.-A. Richard, L. Jean, A. Romieu, M. Massonneau, P. Noack-Fraissignes, P.-Y. Renard, *Org. Lett.* **2007**, *9*, 4853–4855.
[13] L. E. Edgington, A. B. Berger, G. Blum, V. E. Albrow, M. G. Paulick, N. Lineberry, M. Bogyo, *Nat. Med.* **2009**, *15*, 967–973.
[14] J. R. Lakowicz, Principles of Fluorescence Spectroscopy, Kluwer Academic/Plenum Publishers, New York **1999**.

[15] W. S. Hummers Jr., R. E. Offeman, *J. Am. Chem. Soc.* **1958**, *80*, 1339–1339.
[16] Q. Mei, K. Zhang, G. Guan, B. Liu, S. Wang, Z. Zhang, *Chem. Commun.* **2010**, *46*, 7319–7321.
[17] G. Eda, Y. Y. Lin, C. Mattevi, H. Yamaguchi, H. A. Chen, I. Chen, C. W. Chen, M. Chhowalla, *Adv. Mater.* **2010**, *22*, 505–509.
[18] Z. Luo, P. M. Vora, E. J. Mele, A. Johnson, J. M. Kikkawa, *Appl. Phys. Lett.* **2009**, *94*, 1119091–1119093.
[19] K. P. Loh, Q. Bao, G. Eda, M. Chhowalla, *Nat. Chem.* **2010**, *2*, 1015–1024.
[20] T. Gokus, R. Nair, A. Bonetti, M. Bohmler, A. Lombardo, K. Novoselov, A. Geim, A. Ferrari, A. Hartschuh, *ACS Nano* **2009**, *3*, 3963–3968.
[21] M. Roy, T. S. Kusurkar, S. K. Maurya, S. K. Meena, S. K. Singh, N. Sethy, K. Bhargava, R. K. Sharma, D. Goswami, S. Sarkar, *3 Biotech* **2013**, *3*, 1–9.
[22] E. Morales-Narváez, A. Merkoçi, *Adv. Mater.* **2012**, *24*, 3298–3308.
[23] D. Pan, J. Zhang, Z. Li, C. Wu, X. Yan, M. Wu, *Chem. Commun.* **2010**, *46*, 3681–3683.
[24] S. Zhu, J. Zhang, C. Qiao, S. Tang, Y. Li, W. Yuan, B. Li, L. Tian, F. Liu, R. Hu, *Chem. Commun.* **2011**, *47*, 6858–6860.
[25] C. J. Shih, S. Lin, R. Sharma, M. S. Strano, D. Blankschtein, *Langmuir* **2012**, *28*, 235–241.
[26] F. Liu, J. Y. Choi, T. S. Seo, *Biosens. Bioelectron.* **2010**, *25*, 2361–2365.
[27] X. Sun, Z. Liu, K. Welsher, J. T. Robinson, A. Goodwin, S. Zaric, H. Dai, *Nano Res.* **2008**, *1*, 203–212.
[28] J. H. Jung, D. S. Cheon, F. Liu, K. B. Lee, T. S. Seo, *Angew. Chem. Int. Ed.* **2010**, *49*, 5708–5711.
[29] C. H. Lu, H. H. Yang, C. L. Zhu, X. Chen, G. N. Chen, *Angew. Chem.* **2009**, *121*, 4879–4881.
[30] J. Balapanuru, J. X. Yang, S. Xiao, Q. Bao, M. Jahan, L. Polavarapu, J. Wei, Q. H. Xu, K. P. Loh, *Angew. Chem.* **2010**, *122*, 6699–6703.
[31] H. Jang, Y. K. Kim, H. M. Kwon, W. S. Yeo, D. E. Kim, D. H. Min, *Angew. Chem.* **2010**, *122*, 5839–5843.
[32] M. Zhang, B.-C. Yin, W. Tan, B.-C. Ye, *Biosens. Bioelectron.* **2011**, *26*, 3260–3265.
[33] Y. Wen, C. Peng, D. Li, L. Zhuo, S. He, L. Wang, Q. Huang, Q.-H. Xu, C. Fan, *Chem. Commun.* **2011**, *47*, 6278–6280.
[34] X.-H. Zhao, R.-M. Kong, X.-B. Zhang, H.-M. Meng, W.-N. Liu, W. Tan, G.-L. Shen, R.-Q. Yu, *Anal. Chem.* **2011**, *83*, 5062–5066.
[35] Y. Piao, F. Liu, T. S. Seo, *Chem. Commun.* **2011**, *47*, 12149–12151.
[36] T. Feng, D. Feng, W. Shi, X. Li, H. Ma, *Mol. Biosys.* **2012**, *8*, 1441–1445.
[37] K. A. Mkhoyan, A. W. Contryman, J. Silcox, D. A. Stewart, G. Eda, C. Mattevi, S. Miller, M. Chhowalla, *Nano Lett.* **2009**, *9*, 1058–1063.
[38] M. B. M. Krishna, N. Venkatramaiah, R. Venkatesan, D. N. Rao, *J. Mater. Chem.* **2012**, *22*, 3059–3068.
[39] J. J. Brege, C. Gallaway, A. R. Barron, *J. Phys. Chem. C* **2007**, *111*, 17812–17820.
[40] K. Kessenbrock, V. Plaks, Z. Werb, *Cell* **2010**, *141*, 52–67.
[41] E. I. Deryugina, J. P. Quigley, *Cancer Metastasis Rev.* **2006**, *25*, 9–34.
[42] J. Seltzer, K. Akers, H. Weingarten, G. Grant, D. McCourt, A. Eisen, *J. Biol. Chem.* **1990**, *265*, 20409–20413.
[43] Z. Liu, J. T. Robinson, X. Sun, H. Dai, *J. Am. Chem. Soc.* **2008**, *130*, 10876–10877.
[44] D. Feng, Y. Zhang, T. Feng, W. Shi, X. Li, H. Ma, *Chem. Commun.* **2011**, *47*, 10680–10682.
[45] Z. Xia, Y. Xing, M.-K. So, A. L. Koh, R. Sinclair, J. Rao, *Anal. Chem.* **2008**, *80*, 8649–8655.
[46] E. Song, D. Cheng, Y. Song, M. Jiang, J. Yu, Y. Wang, *Biosens. Bioelectron.* **2013**, *47*, 445–450.